



IAS-INSA-NASI
Summer Research Fellowship Programme 2024

**STUDY OF ACCRETION PROCESSES
ACROSS DIFFERENT MODELS**
(8-week report)

Submitted by

Gunjan Jain
Indian Institute of Technology, Guwahati
Application No. : PHYS1939



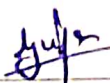
Under the guidance of

Dr. Indranil Chattopadhyay
Aryabhatta Research Institute of observational sciences, Nainital



DECLARATION

I, Gunjan Jain, an MSc student at IIT Guwahati, hereby declare that the material given in this report titled "Study of Accretion Processes Across Different Models" is my original work under the supervision of Dr. Indranil Chattpadhyay and has not been submitted for award in any degree, diploma fellowship or associateship. There is no plagiarism; all data sources, references, and contributions from others have been appropriately recognized.



Gunjan Jain
SRFP 2024



Dr. Indranil Chattpadhyay
Scientist, ARIES

Place : ARIES, Nainital

Date : 10/07/2024

ACKNOWLEDGEMENTS

I would like to thank my adviser, Indranil Chattopadhyay, and his PhD students, Priyesh Kumar Tripathi and Sanjit Debnath, for their continuous support, patience, and advice during this research. Their knowledge and insights were significant in the completion of this project.

I also want to thank my fellow project members, who helped me during my stay at ARIES. This will surely provide valuable experience for my future studies.

I thank my family for their unfailing support and understanding during this time. Their belief in me helped me stay motivated and focused.

I thank the management of ARIES for allowing me to use all available resources, providing lodging and making my stay comfortable.

Finally, I am grateful to science academies for providing the financial support necessary to carry out this research.

ABSTRACT

This report explores the accretion processes in astrophysical contexts. The concept of accretion in astrophysics is important to comprehend as it explains energy production in many celestial systems. In this report, we discussed about steady, spherically symmetric accretion for non-rotating black holes, first with Newtonian potential (Bondi accretion) and later with a pseudo-Newtonian potential (Paczyński–Wiita). Further, we have explained accretion due to pseudo-Newtonian potential known as Artemova potential for a rotating black hole. We also included a comparative analysis at the conclusion.

Contents

| | |
|---|-----------|
| 1 Introduction | 1 |
| 1.1 Why Accretion is Important? | 1 |
| 1.2 Flow of Accreting Matter | 1 |
| 1.3 Plasma concepts | 2 |
| 2 Spherically Symmetric Accretion with Newtonian Potential | 3 |
| 2.1 Formula Derivation | 3 |
| 2.2 Methodology | 6 |
| 2.3 Results | 7 |
| 3 Accretion flow with Paczyński–Wiita Potential | 10 |
| 3.1 Formula Derivation | 10 |
| 3.2 Methodology | 11 |
| 3.3 Results | 12 |
| 4 Accretion flow with Artemova Potential | 13 |
| 4.1 Formula Derivation | 14 |
| 4.2 Methodology | 15 |
| 4.3 Results | 16 |
| 5 Introducing Small Angular Momentum | 17 |
| 5.1 Angular momentum in Newtonian Potential | 17 |
| 5.2 Angular momentum in Paczyński–Wiita Potential | 19 |
| 6 Conclusion | 21 |
| References | 22 |

1 Introduction

Accretion is the process of matter accumulating onto a compact object. This matter, typically composed of gas and dust from the interstellar medium, can form a disc around the central object, which may be a black hole, neutron star, white dwarf, or other types of star. In binary systems, one body, such as a star or galaxy, accretes matter from its companion body, leading to various astrophysical phenomena.

1.1 Why Accretion is Important?

Gravitational potential energy obtained from material accreting onto a gravitating body is a major source of power. This potential energy gets converted into kinetic energy and then into thermal energy, this hot and ionised gas radiates this energy in form of electromagnetic radiation. This energy is given by

$$\Delta E = \frac{GMm}{R},$$

where G is the gravitational constant. Accretion efficiency depends upon the compactness ($\frac{M}{R}$) of the object. For fixed compactness, the luminosity of that object depends on the accretion rate (how fast matter is getting accreted). For steady, spherically symmetric accretion while balancing the inward pull of gravity on protons with outward radiation pressure on electrons, any object can have a maximum luminosity that we call the Eddington limit or Eddington luminosity.

$$\frac{GMm_p}{r^2} = \frac{L\sigma_T}{4\pi cr^2},$$
$$L_{Edd} = 4\pi GMm_p c / \sigma_T.$$

where m_p - the mass of the proton, σ_T - Thomson scattering cross-section, and if S is radiant energy flux, then outward radial force is $\frac{\sigma_T S}{c}$. When luminosity exceeds this limit, it leads to more photons getting generated, radiation pressure will exceed gravitational pull, and accretion will stop. Now, other factors, like nuclear burning, will be responsible for inducing luminosity, which in turn causes the outer layers of the star to begin to fly off[1].

1.2 Flow of Accreting Matter

All accreting matter is in gaseous form constituting electrons and ions that interact with each other by collisions. For lengthscales that are much greater than the mean

free path, it can be considered that particles have Maxwell-Boltzmann distribution of velocities. We consider gas as a continuous fluid having velocity \mathbf{v} , density ρ , pressure P , and temperature T .

Three conservation laws of gas dynamics, conservation of mass (1.1), conservation of momentum (1.2), and conservation of energy (1.3) with equation state (1.4) can describe dynamics of accretion flow[1].

$$\frac{\partial \rho}{\partial t} + \nabla \cdot (\rho \mathbf{v}) = 0, \quad (1.1)$$

$$\rho \frac{\partial \mathbf{v}}{\partial t} + \rho (\mathbf{v} \cdot \nabla) \mathbf{v} = -\nabla P + \mathbf{f}. \quad (1.2)$$

This eq is also called the Euler equation, where \mathbf{f} can be an external force like gravity.

$$\frac{\partial}{\partial t} \left(\frac{1}{2} \rho v^2 + \rho \epsilon \right) + \nabla \cdot \left[\left(\frac{1}{2} \rho v^2 + \rho \epsilon + P \right) \mathbf{v} \right] = \mathbf{f} \cdot \mathbf{v} - \nabla \cdot \mathbf{F}_{rad} - \nabla \cdot \mathbf{q}. \quad (1.3)$$

Here $\frac{1}{2} \rho v^2$ is kinetic energy per unit volume, $\rho \epsilon$ is internal or thermal energy per unit volume. The second term on the right-hand side is radiative flux, which gives the rate at which radiant energy is lost or gained after emission or absorption by unit volume of gas, and the third term is the conductive flux of heat, \mathbf{q} that can be omitted as temperature gradients are small enough.

When m_H is mass of hydrogen atom and μ is mean mass per particle of gas in units of m_H , perfect gas law:

$$P = \frac{\rho K T}{\mu m_H}. \quad (1.4)$$

In this report, we have analyzed accretion for the steady spherically symmetric case with Newtonian potential, then with pseudo-Newtonian potential for the non-rotating black hole, and lastly with Artemova potential for a rotating black hole. Which we will be covering in the next sections.

1.3 Plasma concepts

Plasma in the accretion disc plays a crucial role in the dynamics of accretion and energy release. We use concepts of plasma in our study of accretion whenever we want to consider the behavior of gas on length comparable to the mean free path. Plasma is a mixture of electron gas and ion gas that interact with each other via

coulomb force. Plasma has unique behavior due to its long-range nature of the coulomb force and mass disparity inside the gas.

Plasma must always be charge neutral, which means densities of ions and electrons at any point should be equal, a small imbalance creates a very large electric field, and then plasma particles move to restore this neutrality and induce plasma oscillations[1].

High-velocity particles, like ions or high-energy electrons that fall into an accreting star, lose their energy through coulomb interactions with ions and electrons in the plasma. The rate of energy loss depends upon the density of plasma, higher density leads to higher collisions and greater energy loss. Due to this interaction, they emit electromagnetic radiation known as bremsstrahlung radiation. Many times, these particles undergo spiral or circular motion because of the magnetic field of accreting matter and emit synchrotron radiation. These radiations contribute to the spectrum emitted by the accretion disc and the heating of the disc that influence the dynamics and structure of the disc.

2 Spherically Symmetric Accretion with Newtonian Potential

The problem of steady, spherically symmetric accretion was first studied by Bondi (1952) and is known as Bondi accretion. Here we consider accreting matter falling directly into a non-rotating black hole of mass M from all directions, taking it at rest with respect to gas[2].

2.1 Formula Derivation

To solve the problem mathematically, we take spherical coordinates with the origin at the centre of the object, fluid variables are independent of θ, ϕ . We consider only the radial component of gas velocity ($v = v_r$). For steady-state $\frac{\partial}{\partial t}$ is zero. For steady flow, the continuity equation reduces to

$$\frac{1}{r^2} \frac{d}{dr} (r^2 \rho v) = 0. \quad (2.1)$$

This integrates to $r^2 \rho v = constant$. Hence, our constant accretion rate:

$$\dot{M} = 4\pi r^2 \rho v, \quad (2.2)$$

and if $f = -\frac{GM\rho}{r^2}$, Euler equation reduces to

$$v \frac{dv}{dr} + \frac{1}{\rho} \frac{dP}{dr} + \frac{GM}{r^2} = 0. \quad (2.3)$$

After integrating it with respect to r , we get energy that remains constant,

$$\frac{v^2}{2} + \int \frac{dP}{\rho} - \frac{GM}{r} = \text{constant} = E. \quad (2.4)$$

Polytropic relation between pressure and density for an ideal gas:

$$P = K\rho^\gamma, \quad (2.5)$$

$K = \text{constant}$,

$\gamma = \text{adiabatic index}$,

$\gamma = 1$ for isothermal case,

$\frac{4}{3} \leq \gamma \leq \frac{5}{3}$ for adiabatic case.

$$a^2 = \frac{dP}{d\rho} = \frac{\gamma P}{\rho}, \quad (2.6)$$

where a is the sound speed that is constant in the isothermal case due to constant temperature, but in the adiabatic case, it depends on the position.

$$\frac{dP}{dr} = \frac{dP}{d\rho} \frac{d\rho}{dr} = a^2 \frac{d\rho}{dr},$$

$$\frac{1}{\rho} \frac{d\rho}{dr} = -\frac{1}{vr^2} \frac{d}{dr}(vr^2).$$

Using above relations and eqs 2.1, 2.5, 2.6 in 2.3 we get differential equation:

$$\frac{1}{2} \left(1 - \frac{a^2}{v^2}\right) \frac{dv^2}{dr} = -\frac{GM}{r^2} \left[1 - \frac{2a^2r}{GM}\right]. \quad (2.7)$$

The analytic solution for this equation in isothermal case is

$$\left(\frac{v}{a}\right)^2 - \log\left(\frac{v}{a}\right)^2 = 4\log\left(\frac{r}{r_s}\right) + \frac{4r_s}{r} - c, \quad (2.8)$$

where c is an integration constant, and r_s is the position of sonic point.

From 2.7 we get

$$\frac{dv}{dr} = \frac{\frac{-GM}{r^2} + \frac{2a^2}{r}}{v - \frac{a^2}{v}}. \quad (2.9)$$

Sonic point is a point where particle transitions from subsonic region to supersonic region or vice versa, at sonic point ($r = r_s$) velocity of any particle gets equal to sound speed ($v = a = c_s$) and solutions passing through sonic point are called transonic solutions.

The relation between sonic point and sound speed at sonic point:

$$2c_s^2 = \frac{GM}{r_s}. \quad (2.10)$$

At r_s , $\frac{dv}{dr}$ comes out to be of indeterminate form $(\frac{0}{0})$, so to get $\frac{dv}{dr}$ at sonic point we apply L'Hospital's rule.

Isothermal case:

Using relation 2.10 and after applying L'Hospital's rule in 2.9 for the isothermal case, where $a = c_s$ is constant throughout the process, then at the sonic point, we get

$$\frac{dv}{dr} = \pm \frac{c_s}{r_s}. \quad (2.11)$$

For isothermal case, using 2.1 and 2.6, we get energy:

$$E = \frac{v^2}{2} - c_s^2 \log(vr^2) - \frac{GM}{r}. \quad (2.12)$$

Adiabatic case:

Since sound speed is not constant in this case, then

$$\frac{da^2}{dr} = \frac{a^2}{v}(1-\gamma)\frac{dv}{dr} + \frac{2a^2}{r}(1-\gamma). \quad (2.13)$$

After applying L'Hospital's rule in 2.9 and using 2.13, at sonic point

$$\frac{dv}{dr} = \frac{\frac{4c_s}{r_s}(1-\gamma) \pm \sqrt{\left(\frac{4c_s}{r_s}(1-\gamma)\right)^2 + 4(1+\gamma) \left(\frac{2}{r_s^3} + \frac{2c_s^2}{r_s^2} - 4\gamma\frac{c_s^2}{r_s^2}\right)}}{2(1+\gamma)}. \quad (2.14)$$

We can relate sound speed at any point r with the sound speed at the sonic point via this relation:

$$a = c_s \left(\frac{r_s^2 c_s}{r^2 v}\right)^{\frac{\gamma-1}{2}}. \quad (2.15)$$

Expression for entropy accretion rate in terms of sound speed:

$$\dot{M} = a^{\frac{2}{\gamma-1}} r^2 v. \quad (2.16)$$

For the adiabatic case, we get energy:

$$E = \frac{v^2}{2} + \frac{a^2}{\gamma - 1} - \frac{GM}{r}. \quad (2.17)$$

2.2 Methodology

Our primary objective is to find solutions for the above mentioned differential equations that explain the dynamics of steady, spherically symmetric accretion. Here we have analyzed all possible solutions along with transonic solutions. We have plotted mach number ($M = \frac{v}{a}$) v/s r/r_s curves. In our calculations, we took $GM = 1$ and adiabatic index $\gamma = 1$ in isothermal case and $\gamma = 1.4$ in adiabatic case. For the positive slope, we get wind curve, and for negative slope, we get accretion curve. We have shown type 3, type 4, type 5 and type 6 curves in figure 4.

First, we plotted equation 2.8, which is the analytic solution of 2.7 for the isothermal case. For transonic solutions, we calculated the integration constant, and then, to get other possible solutions, we varied the value of the integration constant and initial guess for velocity. The slope for types 5 and 6 at the sonic point gets infinity, that's why we excluded the data points near the sonic point.

Afterwards, we solved equation 2.9 and 2.11 for the isothermal case and eq 2.9 and 2.14 for the adiabatic case using the RK-4 method and plotted M v/s r/r_s curves. For plotting transonic solutions, we start our integration from the sonic point and get data points in both forward and backward directions.

Similarly, we got values for energy using 2.12 and 2.17 for both the cases and entropy accretion rate using 2.16 for the adiabatic case corresponding to each value of velocity and position.

We only used eq 2.9 for integration to get other kinds of curves. Since energy remains constant over all the curves, we obtained other types of solutions by starting our integration with an energy value and an initial estimate of velocity. For type 3 we did integration in forward direction taking velocity estimate near black hole in subsonic region with slightly less entropy than of transonic curves and type 4, we did the same, but with a velocity estimate in the supersonic region.

Further, for type 5, we did integration by taking velocity estimates near the black hole in the subsonic region with slightly greater entropy than transonic curves. We know that at the sonic point, the slope gets infinity, so to remove that

noise, we plotted the data points first in the subsonic region until it reached a finite slope, and then we moved to the supersonic region and repeated the process for same energy and accretion rate. For type 6, we also applied the same procedure but with an initial velocity estimate far from blackhole,

2.3 Results

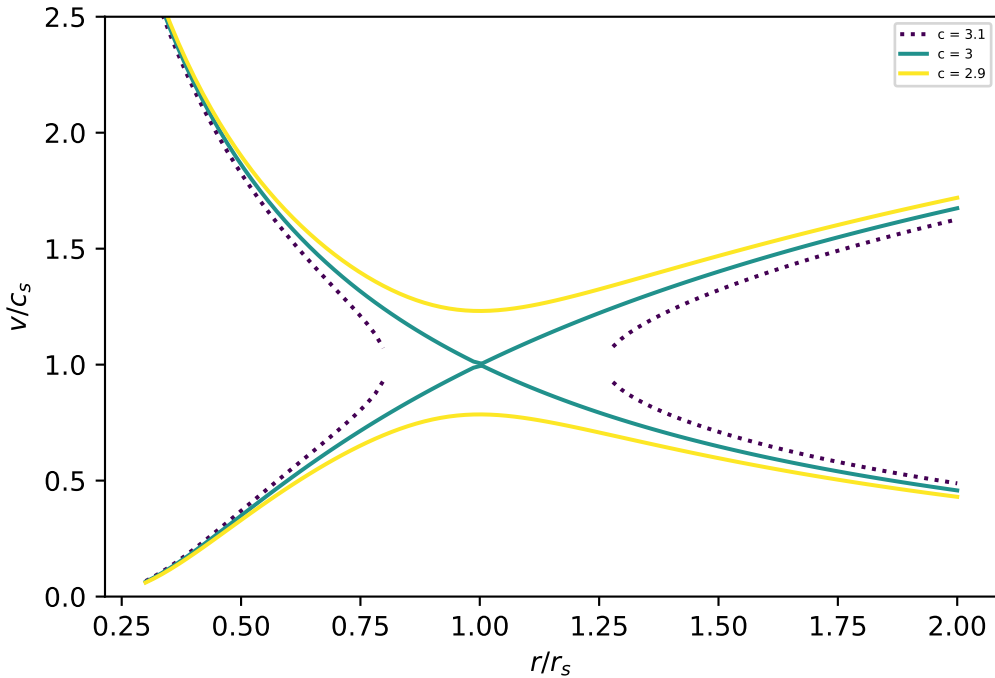


Figure 1: Solutions for eq 2.8

In figure 1, we have plotted solutions of equation 2.8. For transonic solutions, the integration constant comes out to be 3, and for other types, we changed the value of the integration constant by a bit. For type 3 and type 4, we took it as 2.9, and for type 5 and type 6, it was 3.1. At the sonic point, type 5 and type 6 curves have infinite velocity, and type 3 and type 4 curves have extremum points.

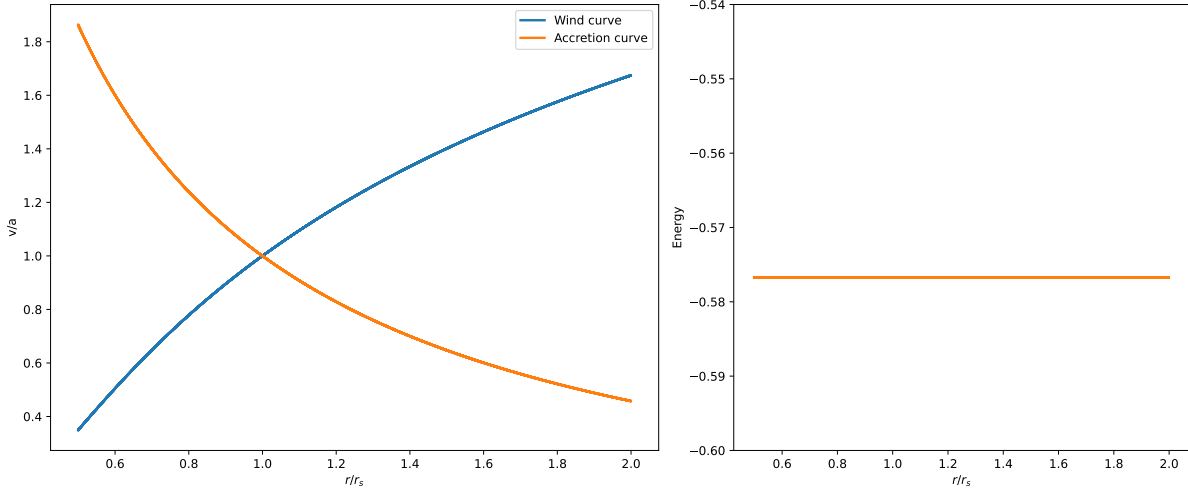


Figure 2: Transonic solutions for eq 2.9 and 2.11 with energy curve

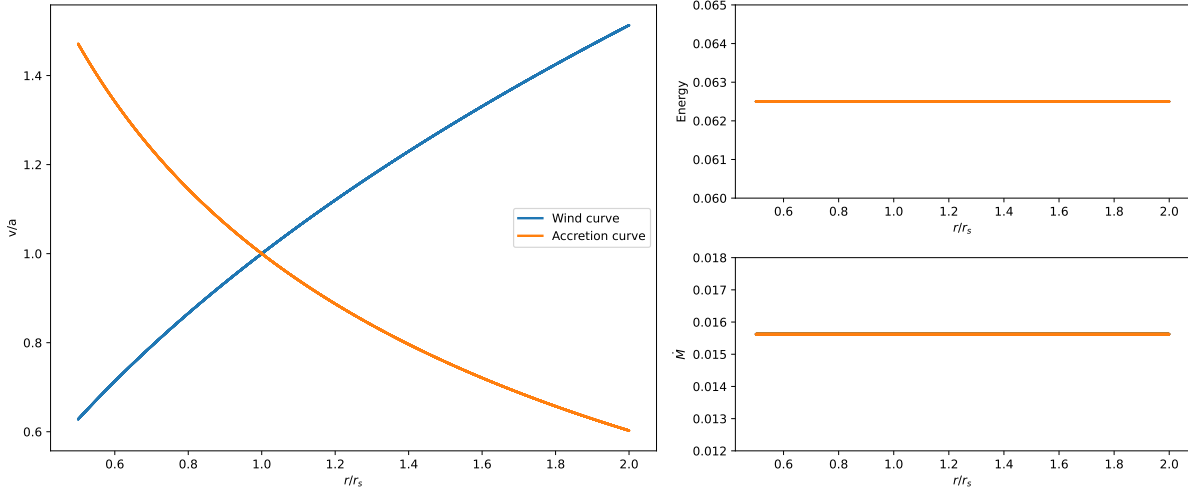


Figure 3: Transonic solutions for eq 2.9 and 2.14 with energy and entropy accretion rate curve

In figure 2, we have shown transonic solutions for the isothermal case and in figure 3 for the adiabatic case. The graph shows that, at a given position, in the adiabatic case, we get less mach number than in the isothermal case. We calculated energy values in isothermal case and verified that it remains constant and the same for both accretion and wind curves. Similarly, we calculated energy and entropy accretion rate for the adiabatic case and verified that they remain constant and same for both accretion and wind curves.

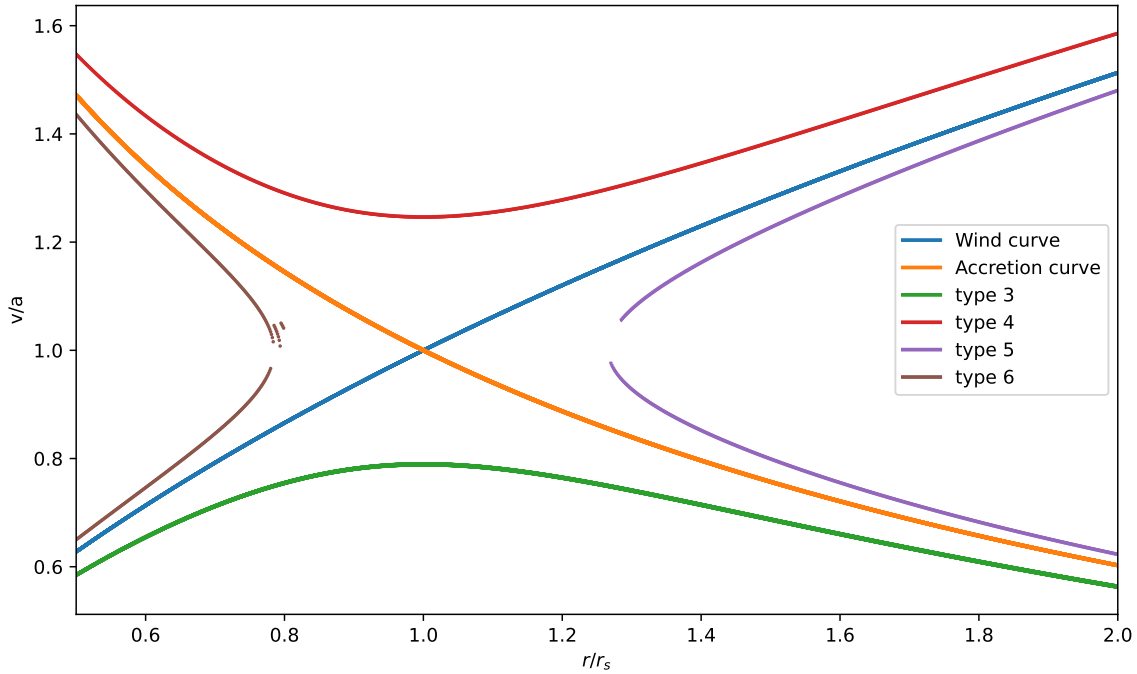


Figure 4: All the types of solutions for eq 3.9

In figure 4, we have shown 6 distinct families of solutions. The first two types are accretion and wind curves passing through the sonic points. Type 5 and type 6 curves, which have an infinite slope at the sonic point and greater entropy accretion rate, do not cover the whole range of r and are double-valued, so they can't be physical solutions. Type 3 and type 4 curves, which have extremum points at the sonic point with less entropy accretion rate, remain subsonic and supersonic throughout the whole range of r , respectively.

We calculated the entropy accretion rate for all the curves and found that it remains constant within one curve, and energy remains constant and the same for all the curves.

3 Accretion flow with Paczyński–Wiita Potential

To counter the relativistic effects around non-rotating blackhole, we replace the Newtonian potential with a pseudo-Newtonian potential known as Paczyński–Wiita potential[3].

$$\phi_{PW} = -\frac{GM}{r - 2r_g}, \quad (3.1)$$

where r_g is gravitational radius as $r_g = \frac{GM}{c^2}$, where c is speed of light. $r_s = 2r_g$ can be considered as the radius of any Schwarzschild (non-rotating black hole). The innermost stable circular orbit for non-rotating blackhole is $6r_g$ [4].

3.1 Formula Derivation

In this case, we are considering spherically symmetric accretion only with the same equation of state as earlier but now in pseudo-Newtonian geometry.

We are considering r in units of $\frac{GM}{c^2}$, then Euler equation:

$$v \frac{dv}{dr} + \frac{1}{\rho} \frac{dP}{dr} + \frac{GM}{(r - 2)^2} = 0. \quad (3.2)$$

After integrating it with respect to r , we get energy that remains constant.

$$\frac{v^2}{2} + \int \frac{dP}{\rho} - \frac{GM}{r - 2} = \text{constant} = E. \quad (3.3)$$

After calculations, we get

$$\frac{dv}{dr} = \frac{\frac{-GM}{(r-2)^2} + \frac{2a^2}{r}}{v - \frac{a^2}{v}}. \quad (3.4)$$

The relation between sonic point and sound speed at sonic point:

$$2c_s^2 = \frac{GMr_s}{(r_s - 2)^2}. \quad (3.5)$$

At r_s , $\frac{dv}{dr}$ comes out to be of indeterminate form $(\frac{0}{0})$, so to get $\frac{dv}{dr}$ at sonic point we apply L'Hospital's rule.

Isothermal case:

Using relation 3.5 and after applying L'Hospital's rule in 3.4 for the isothermal

case, where $a = c_s$ is constant throughout the process, then at the sonic point we get

$$\frac{dv}{dr} = \pm \sqrt{\frac{2GM}{(r_s - 2)^3} - \frac{1}{2r_s(r_s - 2)^2}}. \quad (3.6)$$

For the isothermal case, we get energy:

$$E = \frac{v^2}{2} - c_s^2 \log(vr^2) - \frac{GM}{r - 2}. \quad (3.7)$$

Adiabatic case:

Since sound speed is not constant in this case, then using the relation 2.13 and after applying L'Hospital's rule in 3.4 at sonic point

$$\frac{dv}{dr} = \frac{\frac{4c_s}{r_s}(1 - \gamma) \pm \sqrt{\left(\frac{4c_s}{r_s}(1 - \gamma)\right)^2 + 4(1 + \gamma) \left(\frac{2}{(r_s - 2)^3} + \frac{2c_s^2}{r_s^2} - 4\gamma\frac{c_s^2}{r_s^2}\right)}}{2(1 + \gamma)}. \quad (3.8)$$

Expression for entropy accretion rate in terms of sound speed is

$$\dot{M} = a^{\frac{2}{\gamma-1}} r^2 v. \quad (3.9)$$

For the adiabatic case, we get energy:

$$E = \frac{v^2}{2} + \frac{a^2}{\gamma - 1} - \frac{GM}{r - 2}. \quad (3.10)$$

All the other relations remain the same as they were for Newtonian potential.

3.2 Methodology

For PW potential, we have plotted only transonic solutions, following the same method as earlier, solving differential equations 3.4 and 3.6 for the isothermal case and 3.4 and 3.8 for adiabatic case numerically using RK-4 method. Afterwards, we got the values for energy for both the cases and the entropy accretion rate in the adiabatic case.

3.3 Results

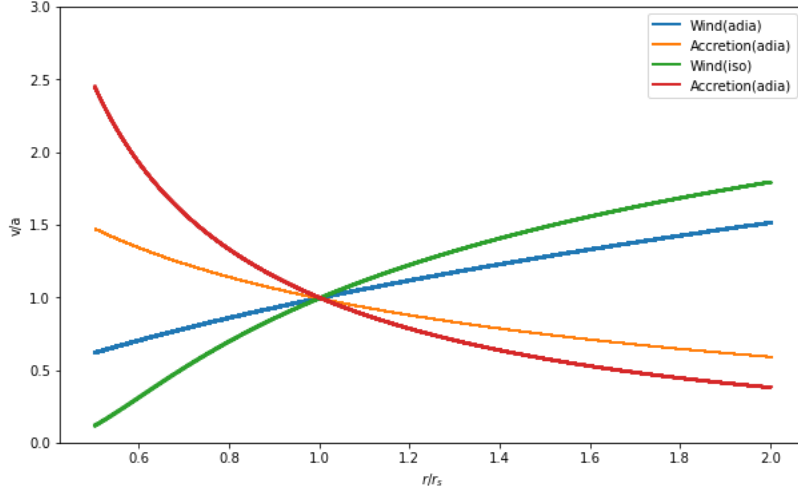


Figure 5: Transonic solutions due to PW potential

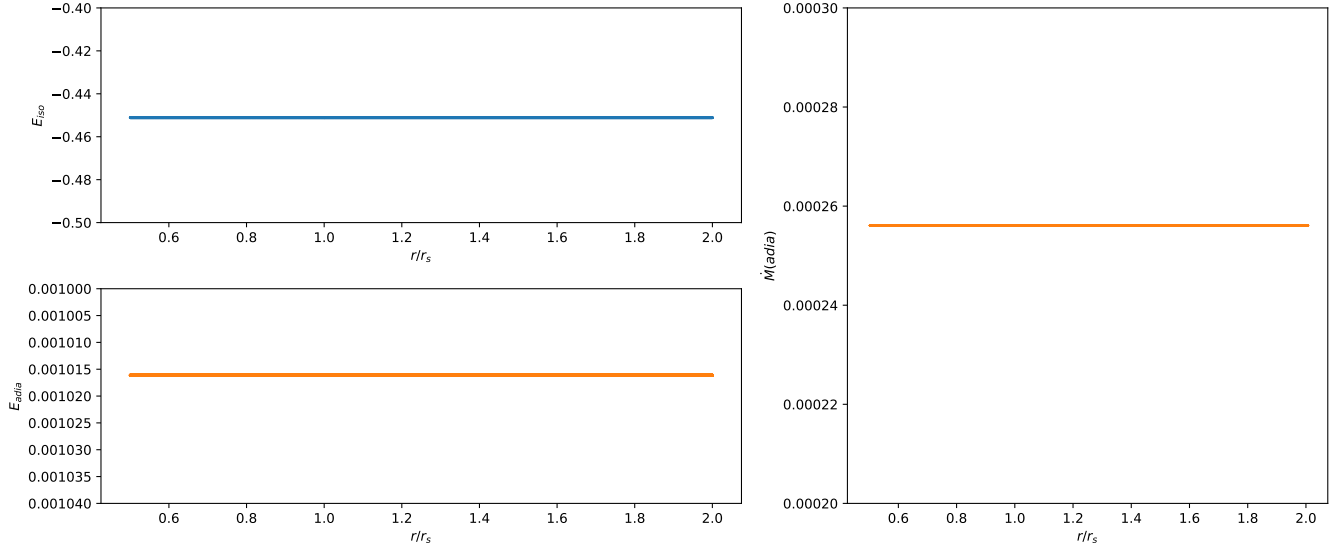


Figure 6: Energy and entropy accretion rate curve in PW potential

In figure 5, we are comparing transonic solutions of an isothermal case due to pseudo-Newtonian potential with the adiabatic case. As it can be seen from the curve, in the isothermal case, the value of the mach number with a given position is higher than in the adiabatic case. Afterwards, in 6, we have verified that energy in both the cases and entropy accretion rate in the adiabatic case remain constant throughout the curves.

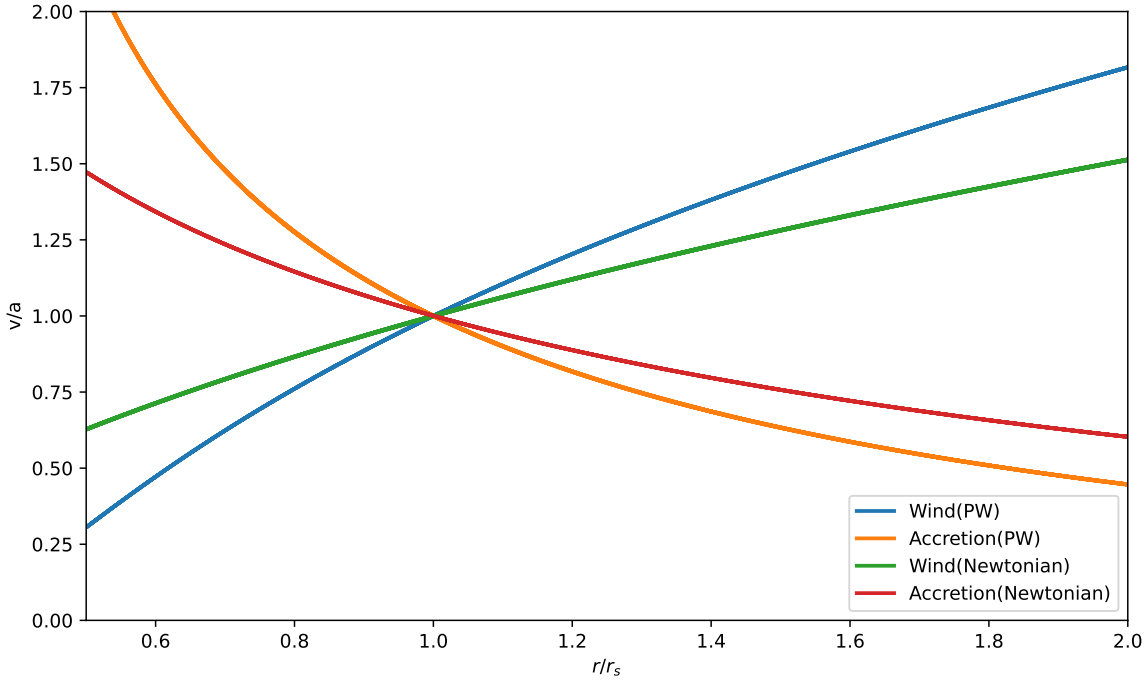


Figure 7: Comparison between Newtonian and pseudo-Newtonian potential

Figure 7 compares the accretion and wind curves resulting from a pseudo-Newtonian potential with those resulting from a Newtonian potential. The velocity of accreting matter near the blackhole is greater in PW potential. Due to higher gravitational potential, in PW potential, accretion becomes more efficient. This is evident from the graph as well, where the accretion curve is steeper, indicating more rapid flow.

4 Accretion flow with Artemova Potential

To describe steady, spherically symmetric accretion around a rotating black hole (Kerr blackhole), we modify the potential such that it should give infinity as it reaches the event horizon. Following is the modified expression for free-fall acceleration:

$$F_5 = -\frac{1}{r^{2-\beta}(r - r_1)^\beta}. \quad (4.1)$$

r_1 is the position of the event horizon, r_{in} is the position of the last stable circular orbit or the innermost edge of the disc, and l is the angular momentum of a black hole. The position of innermost stable circular orbit in a rotating blackhole depends upon its angular momentum. Following are the expressions for r_{in} and r_1 that we get from general relativity.

$$\begin{aligned} r_1 &= 1 + (1 - l^2)^{\frac{1}{2}}, \\ r_{in} &= 3 + Z_2 - [(3 - Z_1)(3 + Z_1 + 2Z_2)]^{\frac{1}{2}}, \\ Z_1 &= 1 + (1 - l^2)^{\frac{1}{3}}[(1 + l)^{\frac{1}{3}} + (1 - l)^{\frac{1}{3}}], \\ Z_2 &= (3l^2 + Z_1^2)^{\frac{1}{2}}, \end{aligned}$$

where exponent $\beta = \frac{r_{in}}{r_1} - 1$. When spin parameter of blackhole $a=0$, Artemova potential will tend to Paczyński–Wiita potential. [4]

4.1 Formula Derivation

In this case, the Euler equation:

$$v \frac{dv}{dr} + \frac{1}{\rho} \frac{dP}{dr} + \frac{1}{r^{2-\beta}(r - r_1)^\beta} = 0. \quad (4.2)$$

After integrating it with respect to r , we get energy that remains constant.

$$\frac{v^2}{2} + \int \frac{dP}{\rho} + \frac{r^{1-\beta}(r - r_1)^{1-\beta}}{r_1(1 - \beta)} = \text{constant} = E. \quad (4.3)$$

After calculations, we get

$$\frac{dv}{dr} = \frac{\frac{-1}{r^{2-\beta}(r-r_1)^\beta} + \frac{2a^2}{r}}{v - \frac{a^2}{v}}. \quad (4.4)$$

The relation between sonic point and sound speed at sonic point is

$$2c_s^2 = \frac{r_s^{-1+\beta}}{(r_s - r_1)^\beta}. \quad (4.5)$$

At r_s , $\frac{dv}{dr}$ comes out to be of indeterminate form $(\frac{0}{0})$, so to get $\frac{dv}{dr}$ at sonic point we apply L'Hospital's rule.

Adiabatic case:

Since sound speed is not constant in this case, then using the relation 2.13 and after applying L'Hospital's rule in 5.4 at sonic point

$$\frac{dv}{dr} = \frac{\frac{4c_s}{r_s}(1-\gamma) \pm \sqrt{\left(\frac{4c_s}{r_s}(1-\gamma)\right)^2 + 4(1+\gamma) \left(\frac{2c_s^2}{r_s^2} - 4\gamma\frac{c_s^2}{r_s^2} - \frac{(\beta-2)r^{\beta-3}}{(r-r_1)^\beta} + \frac{\beta r^{\beta-2}}{(r-r_1)^\beta}\right)}}{2(1+\gamma)}. \quad (4.6)$$

Expression for entropy accretion rate in terms of sound speed:

$$\dot{M} = a^{\frac{2}{\gamma-1}} r^2 v. \quad (4.7)$$

For the adiabatic case, we get energy:

$$E = \frac{v^2}{2} + \frac{a^2}{\gamma-1} + \frac{r^{-1+\beta}(r-r_1)^{1-\beta}}{r_1(1-\beta)}. \quad (4.8)$$

All the other relations remain the same as earlier.

4.2 Methodology

For Artemova potential, we have plotted transonic solutions for adiabatic case by solving differential equations 5.4 and 5.6 using the RK-4 method. For this calculation, we took the value of rotating parameter $a = 0.9998$ and calculated r_{in} , r_1 , and β and used them in further calculations. After that, we calculated energy using 5.8 and entropy accretion rate using 5.7 for each point.

4.3 Results

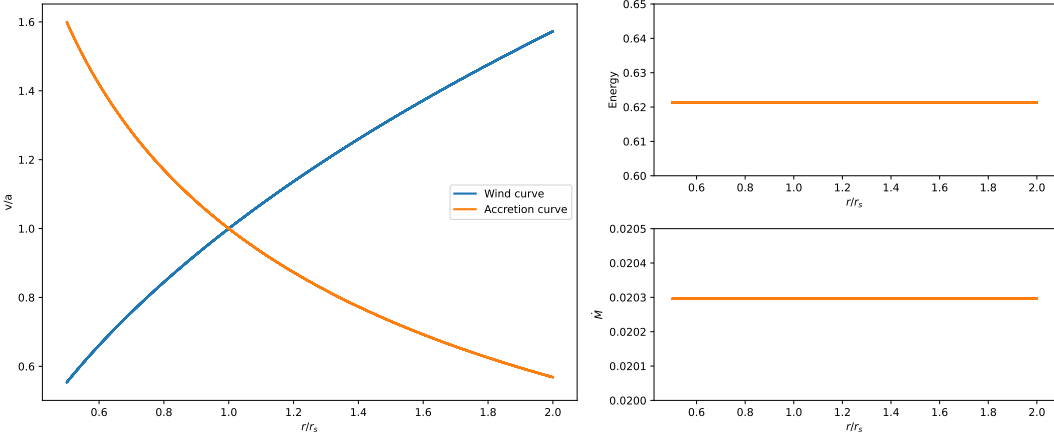


Figure 8: Transonic solution curves due to Artemova potential with energy and entropy accretion rate curves

In figure 8, we have shown transonic solutions due to Artemova potential in the adiabatic case. Afterwards as shown in subplots, we have verified that energy and entropy accretion rate in the adiabatic case remain constant throughout the curve.

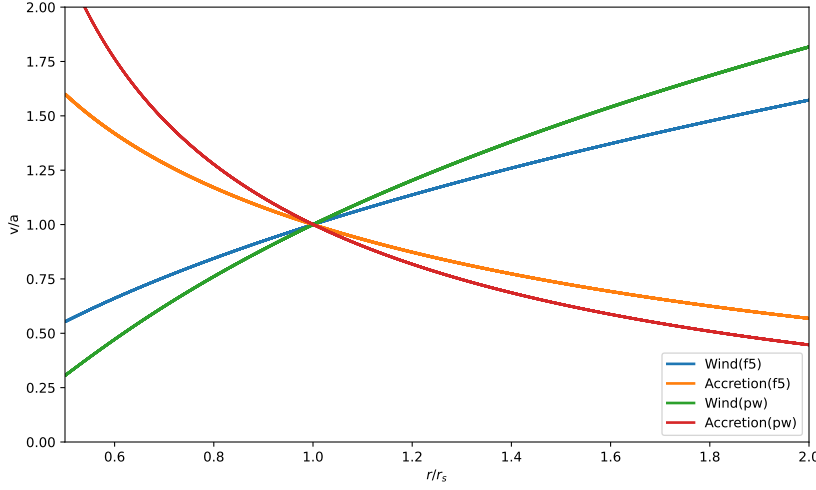


Figure 9: Comparison between Paczyński–Wiita and Artemova potential

In figure 9 we are comparing both pseudo-Newtonian potentials one was for rotating blackhole and one for non-rotating blackhole. Both the potentials were modified considering relativistic effects but it is evident that in non-rotating black-hole case matter accretes more rapidly than in rotating blackhole.

5 Introducing Small Angular Momentum

In this section, we are not considering only spherical accretion but now with small angular momentum, then accreting matter will form a disc-like structure. If we consider a thin disc then v_r and v_ϕ components are non-zero but v_θ component will be zero.

5.1 Angular momentum in Newtonian Potential

Now, if we add centripetal force term with gravity, Euler equation reduces to:

$$v_r \frac{\partial v_r}{\partial r} + \frac{1}{\rho} \frac{dP}{dr} = -\frac{1}{r^2} + \frac{\lambda^2}{r^3}, \quad (5.1)$$

$$v_r \frac{\partial}{\partial r} (v_\phi) + \frac{v_\phi}{r} \frac{\partial v_\phi}{\partial \phi} + \frac{v_r v_\phi}{r} = 0, \quad (5.2)$$

where λ is angular momentum of the gas flow. From equation 5.2 we get $rv_\phi = \lambda = \text{constant}$. After integrating 5.1 with respect to r , for adiabatic case, we get energy that remains constant.

$$\frac{v^2}{2} + \frac{a^2}{\gamma - 1} - \frac{1}{r} + \frac{\lambda^2}{2r^2} = \text{constant} = E. \quad (5.3)$$

For radial velocity after calculations, we get

$$\frac{dv}{dr} = \frac{\frac{-1}{r^2} + \frac{2a^2}{r} + \frac{\lambda^2}{r^3}}{v - \frac{a^2}{v}}. \quad (5.4)$$

The relation between sonic point and sound speed at sonic point is

$$2c_s^2 = \frac{-\lambda^2}{r_s^2} + \frac{1}{r_s}. \quad (5.5)$$

At r_s , $\frac{dv}{dr}$ comes out to be of indeterminate form $(\frac{0}{0})$, so to get $\frac{dv}{dr}$ at sonic point we apply L'Hospital's rule. Then at sonic point

$$\frac{dv}{dr} = \frac{\frac{4c_s}{r_s}(1-\gamma) \pm \sqrt{\left(\frac{4c_s}{r_s}(1-\gamma)\right)^2 + 4(1+\gamma) \left(\frac{2}{r_s^3} + \frac{2c_s^2}{r_s^2} - 4\gamma\frac{c_s^2}{r_s^2} - \frac{3\lambda^2}{r_s^4}\right)}}{2(1+\gamma)}. \quad (5.6)$$

Using 5.3 and 5.5 we can get energy at sonic point in terms of r_s . It is possible for a given energy and λ , there can be more than one sonic point.

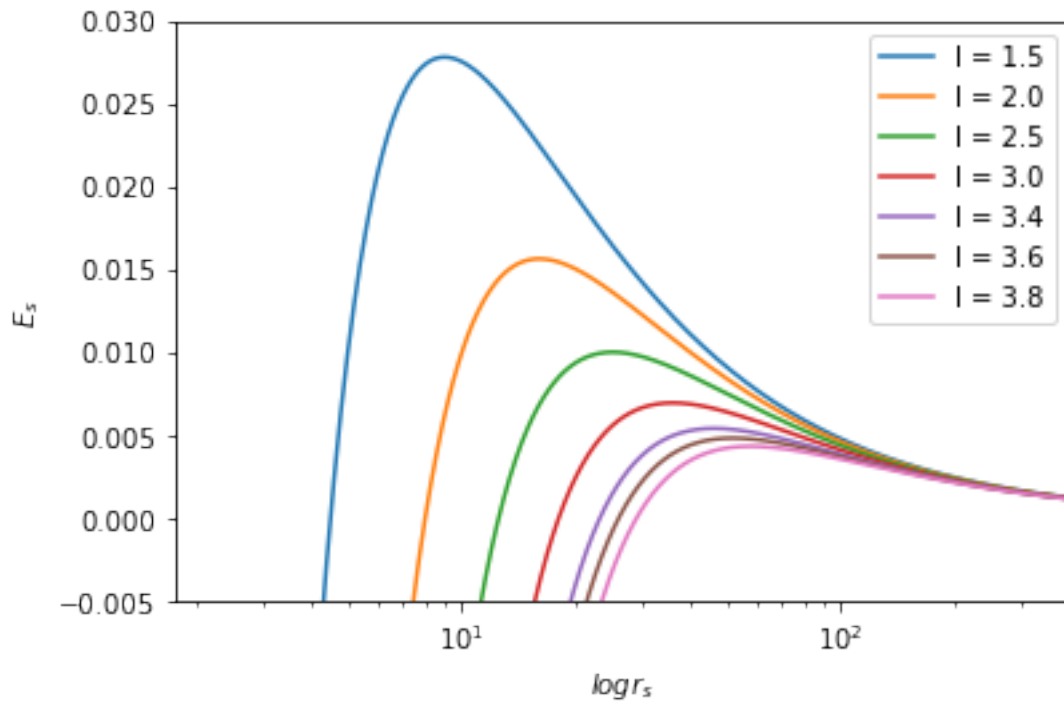


Figure 10: E_s v/s r_s in Newtonian potential

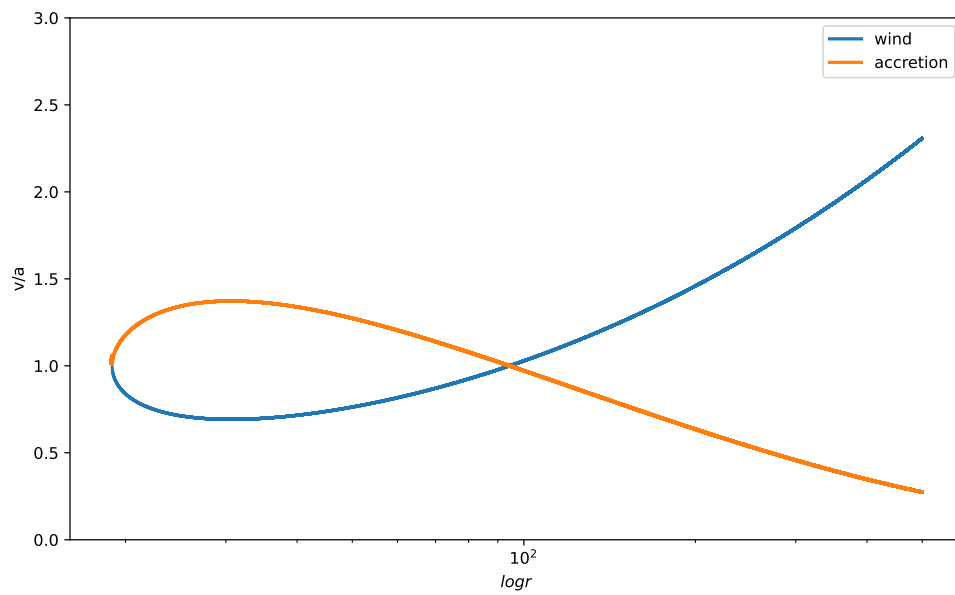


Figure 11: Solution of 5.4 and 5.6 with $\lambda = 3.4$, $E = 0.004$ and outer sonic point $r_s = 94.37867626$

In figure 10 we have shown E_s v/s r_s curves for different values of λ . It is evident from the curve that for lower values of λ in Newtonian potential, we get 2 sonic points for a given energy. When we analysed accretion and wind curves with both inner and outer sonic point, we found that flow is not possible for inner sonic point in Newtonian potential. For outer sonic point also when gas is coming closer to the object even for small angular momentum centripetal force will be so high that it won't reach event horizon.

5.2 Angular momentum in Paczyński–Wiita Potential

Now, if we add centripetal force term with gravity, Euler equation reduces to:

$$v_r \frac{\partial v_r}{\partial r} + \frac{1}{\rho} \frac{dP}{dr} = -\frac{1}{(r-2)^2} + \frac{\lambda^2}{r^3}, \quad (5.7)$$

$$v_r \frac{\partial}{\partial r}(v_\phi) + \frac{v_\phi}{r} \frac{\partial v_\phi}{\partial \phi} + \frac{v_r v_\phi}{r} = 0, \quad (5.8)$$

where λ is angular momentum of the gas flow. From equation 5.8 we get $rv_\phi = \lambda = \text{constant}$. After integrating 5.7 with respect to r , for adiabatic case, we get energy that remains constant.

$$\frac{v^2}{2} + \frac{a^2}{\gamma - 1} - \frac{1}{r-2} + \frac{\lambda^2}{2r^2} = \text{constant} = E. \quad (5.9)$$

For radial velocity after calculations, we get

$$\frac{dv}{dr} = \frac{\frac{-1}{(r-2)^2} + \frac{2a^2}{r} + \frac{\lambda^2}{r^3}}{v - \frac{a^2}{v}}. \quad (5.10)$$

The relation between sonic point and sound speed at sonic point is

$$2c_s^2 = r_s \left(\frac{-\lambda^2}{r_s^3} + \frac{1}{(r_s - 2)^2} \right). \quad (5.11)$$

At r_s , $\frac{dv}{dr}$ comes out to be of indeterminate form $(\frac{0}{0})$, so to get $\frac{dv}{dr}$ at sonic point we apply L'Hospital's rule. Then at sonic point

$$\frac{dv}{dr} = \frac{\frac{4c_s}{r_s}(1-\gamma) \pm \sqrt{\left(\frac{4c_s}{r_s}(1-\gamma)\right)^2 + 4(1+\gamma) \left(\frac{2}{(r_s-2)^3} + \frac{2c_s^2}{r_s^2} - 4\gamma\frac{c_s^2}{r_s^2} - \frac{3\lambda^2}{r_s^4}\right)}}{2(1+\gamma)}. \quad (5.12)$$

Using 5.9 and 5.11 we can get energy at sonic point in terms of r_s . It is possible for a given energy and λ , there can be more than one sonic point.

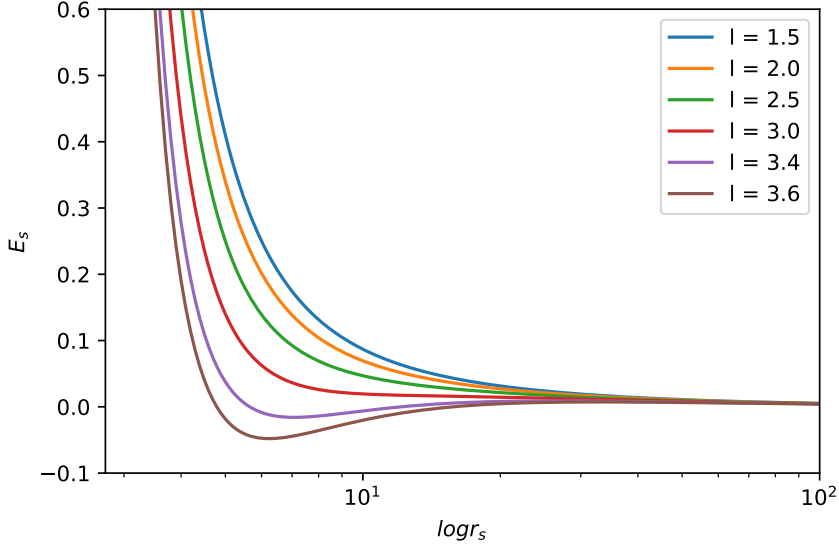


Figure 12: E_s v/s r_s in Paczyński–Wiita potential

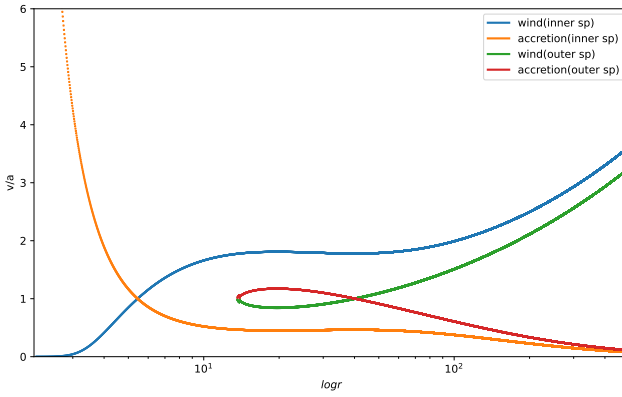


Figure 13: Solution of 5.10 and 5.12 with $\lambda = 3.4$, $E=0.008$ with inner sonic point $r_s=5.44521917$ and outer sonic point $r_s = 40.11081135$

In figure 12, we have shown E_s v/s r_s curves for different values of λ . It is evident from the curve that for $\lambda \geq 3$ in Paczyński–Wiita potential, we get 3 sonic points for a given energy. When we analysed accretion and wind curves with all the sonic points, we found that flow is not possible for middle sonic point and possible for inner and outer sonic points, this leads to formation of shocks, when gas drastically changes its speed from supersonic region to subsonic region and again transitions

through inner sonic point. Furthermore, for outer sonic point entropy accretion rate comes out to be greater than in inner sonic point

6 Conclusion

In this report, we analyzed the accretion process using various models to understand the impact of the gravitational environment on accretion efficiency. Initially, we examined steady, spherically symmetric accretion around a black hole, comparing the Newtonian potential and the pseudo-Newtonian potential for both rotating and non-rotating black holes. A significant part of our analysis focused on comparing transonic solutions, considering both isothermal and adiabatic cases. In every potential, we observed higher Mach numbers in the isothermal case. Energy and entropy accretion rate comes out to be constant for one type of flow, indicating conservation of these quantities.

Through a comparative analysis of Newtonian and pseudo-Newtonian potentials for non-rotating black holes, we concluded that the higher gravitational potential in the PW potential makes accretion more efficient and accounts for relativistic effects. However, the Artemova potential for a rotating black hole proved to be a less accurate approximation.

We then discussed accretion when the gas flow has angular momentum, which introduces a centripetal force that reduces the effect of gravity, preventing matter from falling directly into the object and forming a disc-like structure instead. With angular momentum, we observed that gas flow can have multiple sonic points for the same energy, leading to the formation of shocks and allowing the flow to transition from subsonic to supersonic more than once.

In the future, we can analyze more complex models using the same techniques with improved potential approximations

References

- [1] Juhan Frank, Andrew R King, and Derek Raine. *Accretion power in astrophysics*. Cambridge university press, 2002.
- [2] A Bondi. “On the Properties of Fluorocarbon and Polysiloxane Fluids.” In: *The Journal of Physical Chemistry* 55.8 (1951), pp. 1355–1368.
- [3] Sandip Kumar Chakrabarti. *Theory of transonic astrophysical flows*. World Scientific, 1990.
- [4] Ioulia Vladimirovna Artemova, G Björnsson, and Igor Dmitrievich Novikov. “Modified Newtonian potentials for the description of relativistic effects in accretion disks around black holes”. In: *Astrophysical Journal v. 461*, p. 565 461 (1996), p. 565.